Transactions of the Korean Nuclear Society Autumn Meeting
Goyang, Korea, October 24-25, 2019

Effect of 2-D Plane Graphene Thermal Effusivity on Boiling Heat Transfer with Highly Wettable FC-72

Ji Yong Kim, Kyung Mo Kim, and In Cheol Bang*
Department of Nuclear Engineering., Ulsan National Institute of Science and Technology (UNIST).,
50 UNIST-gil., Ulju-gun., Ulsan., Republic of Korea
**Corresponding author: +82-52-217-2915, +82-52-217-2429, icbang@unist.ac.kr*

1. Introduction

The generation and removal of heat in a thermal - controlled system such as a nuclear power plant is an important issue from the viewpoint of safety and economics. The boiling heat transfer which accompanies the latent heat of working fluid is considered as the most efficient cooling methodology due to low wall superheat. The critical heat flux (CHF), and heat transfer coefficient (HTC) is a key parameter related to the performance of boiling heat transfer. The CHF is considered as upper thermal limit during boiling since the occurrence of CHF accompany sudden increase of wall temperature due to the formation of vapor blanket of heat transfer area. The HTC which is defined as applied heat flux divided by wall superheat represents the efficiency of boiling heat transfer.

The various research studies were made to enhance the boiling CHF and HTC though boiling heat transfer surface modification. These strategies include surface patterning [1,2], formation of porous capillary structures [3,4], and modulation of heater's interfacial/internal properties by deposition and coating of various materials on heat transfer surface [5]–[8].

The discovery of graphene attracts interest from various engineering and science research filed due to superior material properties [9]. The various pool boiling study with graphene material including graphene oxide (GO), and reduced graphene oxide (r-GO) was conducted to investigate the role of graphene's material properties on boiling applications [10]–[13]. The experimental results with graphene material show enhanced CHF, and HTC simultaneously. The reason for the enhancement of boiling heat transfer is attributed to enhanced material thermal properties especially thermal effusivity and activity.

The effect of material thermal properties (thermal effusivity and thermal activity) on boiling heat transfer (CHF, and HTC) was studied by previous researchers [14]–[16]. They observed that enhanced material thermal activity results in enhanced CHF and HTC. They explain that enhanced boiling CHF and HTC was attributed to increased radial heat dissipation which reduces the wall superheat and delay the formation of dry spots.

However, the effect of pristine graphene on boiling heat transfer was limited due to the difficulty of large-scale graphene synthesis. The formation of defects on the graphene sheet during the synthesis process or transferring process degrades the material thermal properties including thermal conductivity [11] since it disrupts the unique structures inside the graphene. The degraded material thermal properties of graphene sheets on the heat transfer surface make hard to analyze the pure graphene thermal properties effects on the boiling performance. Therefore, in this study, we investigate the effect of near-perfect graphene which has defect less than 5% on boiling performance.

2. Experimental Setup

The 2-D saturated pool boiling experiment under atmospheric condition is performed to investigate the effect of near-percent graphene on boiling heat transfer. The schematic configuration of the experimental apparatus is depicted in Fig. 1. The polycarbonate boiling vessel is utilized in this study to visualize the boiling phenomena during the experiment. The copper condenser is used to condensate the working fluid back into the boiling vessel to keep the working fluid level during the experiment. The temperature of working fluid is kept as saturation temperature (56°C) by four cartridge heaters located the bottom side of the boiling vessel. Highly wettable FC-72 is used as working fluid to suppress the effect of surface wettability [11] since FC-72 has low surface tension (0.01 N/m).

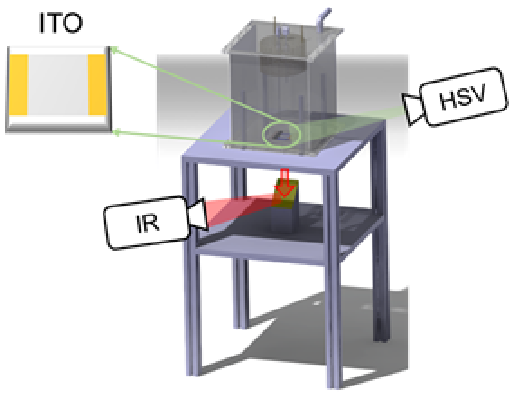

Fig. 1. Schematic configuration of pool boiling experimental apparatus in this study.

The Joule heating method is utilized to increase the power level. The applied heat flux is calculated by applied voltage difference across the ITO specimen (V), and electric current (I) inside the circuit, and effective heat transfer area (A_s) as depicted in equation (1). The standard resistance of 0.01Ω is utilized to calculate the electric current followed by equation (2). All the data is recorded by the data acquisition system (DAS, Agilent 34980A). The step-wise power escalation with 10-kW/m^2 increment is applied to increase the power level during the experiment. The high-speed video camera (HSV), and infrared (IR) camera are utilized to visualize the boiling phenomena and temperature filed respectively.

$$q'' = \frac{(V \times I)}{A} \tag{1}$$

$$I = \frac{V_R}{0.001\ \Omega} \tag{2}$$

2.1 *Fabrication of ITO Heater*

The indium tin oxide (ITO) material is used as heater material in this study to visualize the temperature filed. The sapphire substrate (50mm x 50mm) with 1mm thickness is used as a base material of ITO heater since it has transparent characteristics in the IR range. The ITO is deposited on the sapphire substrate (32mm x 50mm) by E-beam evaporation. The thickness of the ITO deposition layer is determined as ~700nm to guarantee the opaqueness of the IR range during the experiment [17]. The gold electrode (9mm x 32mm) with ~100nm is deposited on ITO substrate to lead the electric current into ITO. Finally, the effective heat transfer area is determined as 32mm x 32mm. The detailed procedure and geometry information can be found in Fig. 2.

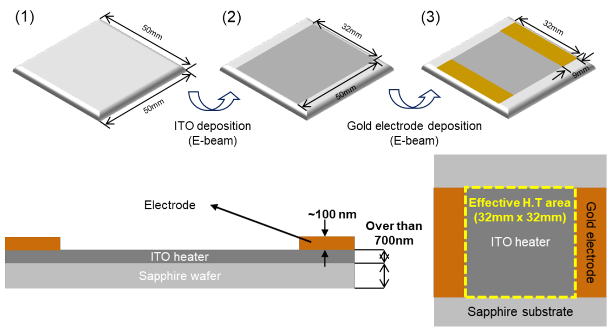

Fig. 2. The procedure for ITO heater fabrication (up) and corresponding deposition thickness and geometry (down).

2.3 Manufacturing of Graphene Deposited Heater and Characterization

The large scale near-perfect graphene was synthesized and transferred on ITO heater surface (by Graphene Square). The graphene is grown on Cu foil by chemical vapor deposition (CVD) method. Then, PMMA coating is applied on graphene grown surface for transferring purpose and forms PMMA-graphene composite. After thermal treatment and etching of Cu foil, PMMA-graphene composite is transferred on the ITO heater surface (32mm x 32mm) and thermal annealing is applied to solder the PMMA-graphene composite on the ITO heater surface. Finally, the PMMA is removed by acetone. The synthesized graphene on the ITO heater can be found in Fig 3.

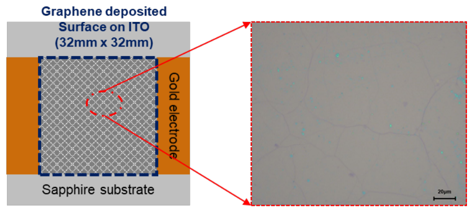

Fig. 3. Schematic image of graphene deposited heat surface (left), and SEM image of 500 times magnified graphene sheet on ITO heater surface (right).

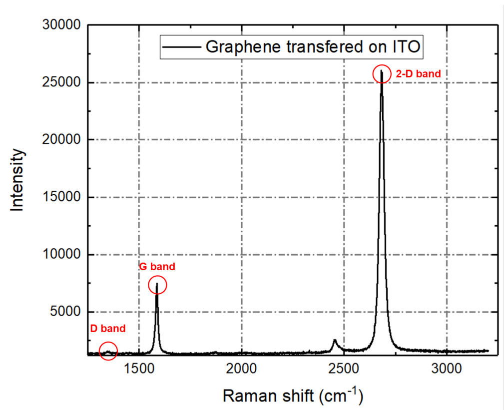

Fig. 4. Measured Raman spectroscopy intensity data for defect characterization.

The Raman spectroscopy is the most widely used method to define the surface characteristics of graphene deposited surface [13]. The representative peaks observed in Raman spectroscopy of graphene is the G-peak, D-peak, and the 2-D peak. The G-peak is the result of sp^2 hybridized bonding of carbon in graphene. The width and position of G-peak give information about layer thickness of pristine graphene. In this study, G-peak is observed at the wavenumber of ~ 1586cm^{-1}. The D-peak represent the degree of defect inside the graphene. In this study, D-peak is observed at the wavenumber of ~ 1344cm^{-1} and the intensity of D-peak is negligible compared to other bands. This result guarantees the synthesized graphene in this study is pristine or near-perfect. The Raman spectroscopy intensity ratio between D-peak and G-peak gives information about amounts of defects inside the graphene. The degree of oxidation and reduction of the graphene sheet also can be confirmed by measuring the intensity ratio between D-peak and G-peak, these values are constantly measured after each case of the experiment. The 2-D peak is secondary D-peak and resulted from phonon lattice vibrations. The 2-D peak is observed at $2684 cm^{-1}$. The measured Raman spectroscopy results show good agreement with reported values in literature.

2.4 Preliminary Result and Discussion

The temperature field of heater surface experiences transient conduction during boiling of working fluid due to cyclic formation and detachment of bubbles on the heater surface. The transient heat transfer is governed by material thermal diffusivity (α) and effusivity (*e*) of heater material. The definition of thermal diffusivity (α) and effusivity (*e*) is depicted in equation (4,5) respectively.

$$\alpha = \frac{k}{\rho c_p} \quad (4)$$

$$e = \sqrt{\rho c_p k} \quad (5)$$

The boiling curve for bare ITO heater and conceptual line for graphene deposited heater surface are depicted in Fig. 5. The CHF of bare ITO heater was observed as 140 kW/m^2. The enhanced HTC and CHF values are expected on the graphene sheet deposited heater surface as shown in Fig 5. The enhanced thermal effusivity of heater surface will dissipate more heat on the heater surface and will results in enhanced CHF due to the delaying of the formation of dry-spot. The reduced wall superheat due to superior thermal effusivity will result in enhanced HTC and early occurrence of onset of nucleate boiling point. The temperature profile change due to enhanced thermal diffusivity is expected and will be analyzed by visualization of the temperature field of bare and graphene deposited surface.

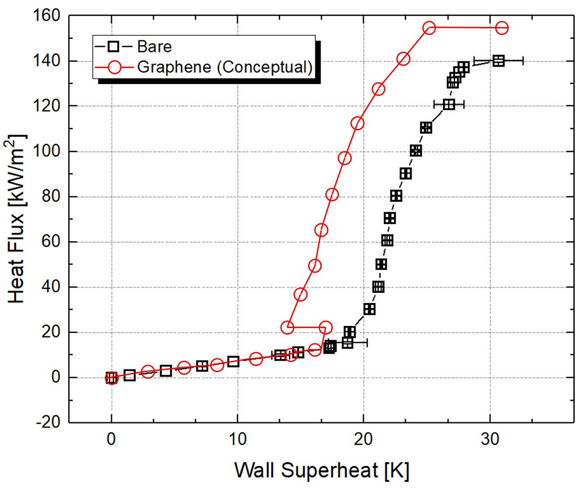

Fig. 5. Pool boiling curve results with highly wettable FC-72 for bare ITO heater and graphene deposited heat surface (conceptual).

3. Summary and Further Work

The study of saturated pool boiling experiment with highly wettable FC-72 on bare ITO heater and near-perfect graphene sheet deposited surface are depicted in this paper. The experimental result of near-perfect graphene sheet deposited surface and analysis of temperature field variation based on material thermal properties will be performed.

NOMENCLATURE

A	*area*
I	*electric current*
V	*voltage difference*
q″	*heat flux*
e	*thermal effusivity*
k	*thermal conductivity*
c_p	*specific heat capacity*

Greek letters

α	*thermal diffusivity*
σ	*surface tension*
ρ	*density*

Subscripts

S	*surface*
R	*standard resistance*

ACKNOWLEDGEMENT

This research was supported by Basic Science Research Program through the National Research Foundation of Korea (NRF) funded by the Korea government (MSIT) (No. 2017R1A2B2008031).

REFERENCES

[1] H. Seo, Y. Lim, H. Shin, and I. C. Bang, Effects of hole patterns on surface temperature distributions in pool boiling, International Journal of Heat and Mass Transfer, Vol. 120, p. 587–596, 2018.
[2] Y. Liu, J. Tang, L. Li, Y. N. Shek, and D. Xu, Design of Cassie-wetting nucleation sites in pool boiling, International Journal of Heat and Mass Transfer, Vol. 132, p. 25–33, 2019.
[3] S. G. Liter and M. Kaviany, Pool-boiling CHF enhancement by modulated porous layer coating: theory and experiment, International Journal of Heat and Mass Transfer, Vol. 44, p. 4287–4311, 2001.
[4] J. Yang and F. B. Cheung, A hydrodynamic CHF model for downward facing boiling on a coated vessel, International journal of heat and flud flow, Vol. 26(3), p. 474–484, 2005.
[5] H. Seo, J. H. Chu, S. Y. Kwon, and I. C. Bang, Pool boiling CHF of reduced graphene oxide, graphene, and SiC-coated surfaces under highly wettable FC-72, International

Journal of Heat and Mass Transfer, Vol. 82, pp. 490–502, 2015.
[6] H. D. Kim and M. H. Kim, Effect of nanoparticle deposition on capillary wicking that influences the critical heat flux in nanofluids, Applied Physics Letter, Vol. 91(1):014104, 2007.
[7] S. J. Kim, I. C. Bang, J. Buongiorno, and L. W. Hu, Effects of nanoparticle deposition on surface wettability influencing boiling heat transfer in nanofluids, Applied Physics Letter, Vol. 89(15):153107, 2006.
[8] G. M. Son, K. M. Kim, and I. C. Bang, Chromia coating with nanofluid deposition and sputtering for accident tolerance, CHF enhancement, International Journal of Heat and Mass Transfer, Vol. 118, pp. 890–899, 2018.
[9] M. Sang, J. Shin, K. Kim, and K. J. Yu, Electronic and Thermal Properties of Graphene and Recent Advances in Graphene Based Electronics Applications, Nanomaterials, Vol. 9(3):374, 2019.
[10] S. D. Park, S. W. Lee, S. Kang, I. C. Bang, J. H. Kim, H. S. Shin, D. W. Lee, and D. W. Lee, Effects of nanofluids containing graphene/graphene-oxide nanosheets on critical heat flux, Applied. Physics. Letter, Vol. 97(2):023103, 2010.
[11] H. Seo, H. D. Yun, S. Y. Kwon, and I. C. Bang, Hybrid Graphene and Single-Walled Carbon Nanotube Films for Enhanced Phase-Change Heat Transfer, Nano Letters., Vol. 16(2), p. 932–938, 2016.
[12] H. S. Ahn, J. M. Kim, T. Kim, S. C. Park, J. M. Kim, Y. Park, D. I. Yu, K. W. Hwang, H. J. Jo, H. S. Park, H. D. Kim, and M. H. Kim, Enhanced heat transfer is dependent on thickness of graphene films: The heat dissipation during boiling, Scientific reports, Vol. 4:6276, 2014.
[13] A. Jaikumar, A. Gupta, S. G. Kandlikar, C. Y. Yang, and C. Y. Su, Scale effects of graphene and graphene oxide coatings on pool boiling enhancement mechanisms, International Journal of Heat and Mass Transfer, Vol. 109, p. 357–366, 2017.
[14] A. A. Watwe and A. Bar-Cohen, The Role of Thickness and Thermal Effusivity in Pool Boiling Chf in Highly-Wetting Liquids, International Heat Trnasfer Conference, p. 183–188, 2019.
[15] M. Arik and A. Bar-Cohen, Effusivity-based correlation of surface property effects in pool boiling CHF of dielectric liquids, International Journal of Heat and Mass Transfer, Vol. 46(20), p. 3755–3764, 2003.
[16] I. Golobic and A. E. Bergles, Effects of Heater-Side Factors on the Saturated Pool Boiling Critical Heat Flux, Experimental Thermal and Fluid Science, Vol. 15(1), p. 43–51, 1997.
[17] I. C. Bang, J. Buongiorno, L.-W. Hu, and H. Wang, Measurement of Key Pool Boiling Parameters in Nanofluids for Nuclear Applications, Journal of Power and Energy Systems, Vol. 2(1), p. 340–351, 2008.